SPECTRAL STUDIES OF SHALLOW EARTHQUAKES AND EXPLOSIONS IN SOUTHERN CALIFORNIA

Peter M. Shearer and Bettina P. Allmann

Institute of Geophysics and Planetary Physics, University of California San Diego

Sponsored by Air Force Research Laboratory

Contract No. FA8718-06-C-0004

ABSTRACT

We compute and analyze *P*-wave spectra from 18,101 earthquakes and 1770 explosions recorded by 196 broadband seismic stations in southern California at epicentral distances of up to 200 km. We use an online waveform database stored on a RAID system at Caltech, which provides complete access to the Southern California Seismic Network (SCSN) seismogram archive. We compute spectra using 1.28 s noise and signal windows, positioned immediately before and after the *P* arrivals. After applying a signal-to-noise cutoff, we process the spectra using an iterative robust least-squares method to isolate source, receiver, and propagation path contributions. This corrects for first-order attenuation structure, as well as near-receiver site effects and any errors in the instrument response functions. Using the earthquake spectra and a simple source model, we compute an empirical Green's function to remove the tradeoff between the source terms and other terms in our model. Our observed earthquake spectra fit reasonably well with a constant stress drop model over a wide range of moment. However, the explosion spectra show significant differences from the earthquake spectra and have generally steeper falloffs at high frequencies. We also compare *P* and *S*-wave amplitudes and find modestly smaller average *S* amplitudes for the explosions compared to the earthquakes. The best earthquake/explosion discriminant is the RMS misfit to an ω^{-2} source model, which works for ~90% of the events.

OBJECTIVES

Routine seismic discrimination between earthquakes and explosions has been a long-standing goal in nuclear test ban treaty research (for a recent review, see Stump et al., 2002). A variety of methods have been employed, including amplitude ratios among regional phases (e.g., Bennett and Murphy, 1986; Wuster, 1993; Plafcan et al., 1997; McLaughlin et al., 2004), spectral studies (e.g., Taylor et al., 1988; Gitterman and van Eck, 1993; Kim et al., 1994; Walter et al., 1995; Gitterman et al., 1998), coda studies (e.g., Su et al., 1991; Hartse et al., 1995), ripple-fire detection schemes (e.g., Hedlin et al., 1990; Smith, 1993; Carr and Garbin, 1998; Hedlin, 1998; Arrowsmith et al., 2006), and other methods (e.g., Musil and Plesinger, 1996; Parolai et al., 2002; Leidig et al., 2004; Tibuleac et al., 2004).

The goal of this project is to systematically analyze and compare source spectra from locally recorded earthquakes and explosions in Southern California (Figure 1) in order to develop new insights into discrimination methods. Advances in data storage and computer capabilities make possible much more extensive analyses than have been performed in the past, which will provide a better picture of the distribution of source spectral properties and amplitudes. By examining tens of thousands of events, we will quantitatively characterize differences between earthquakes and explosions in terms of their spectral content and their *P/S* energy ratios. We also plan to identify and examine anomalous events, in particular earthquakes that may appear like explosions in spectral discrimination methods in order to determine how common they are and whether alternate discrimination techniques can be applied.

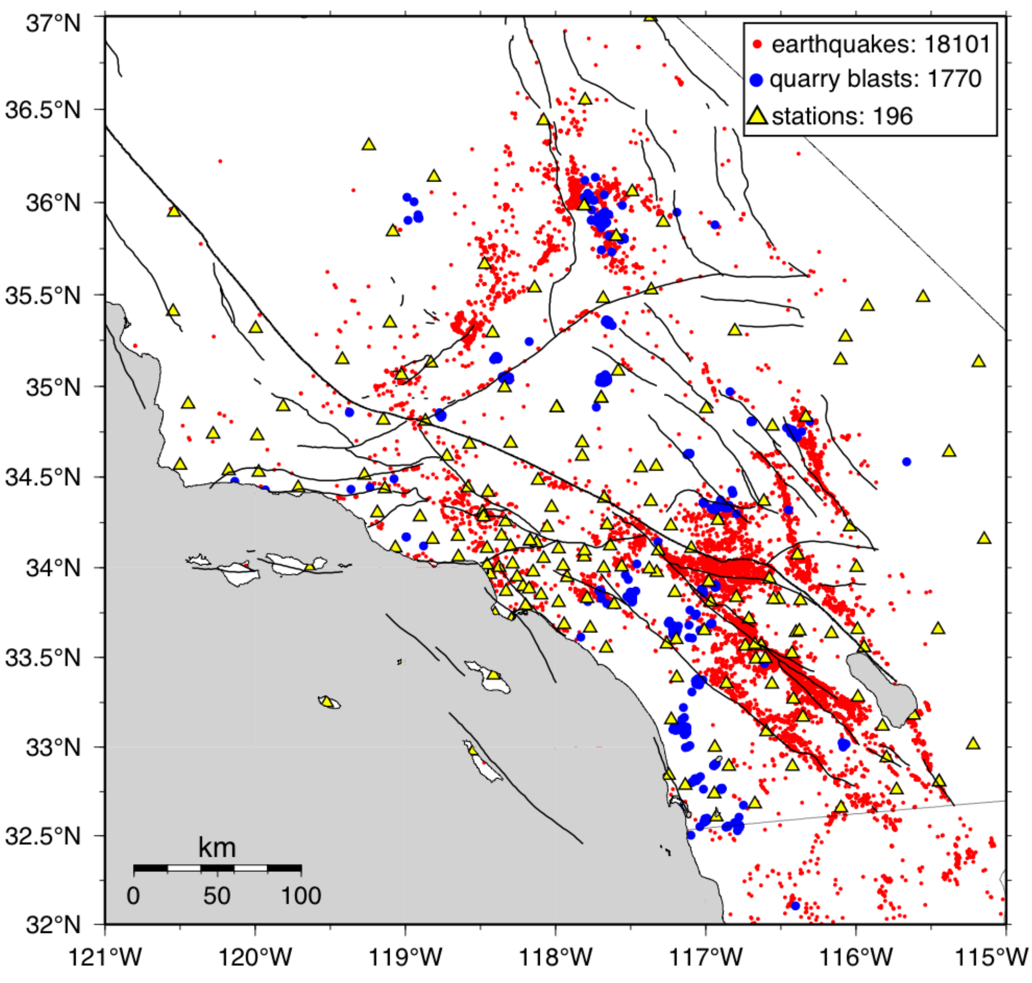

Figure 1. Locations of 18,101 earthquakes (red) and 1770 explosions (blue) in southern California from 2000 to 2005 as recorded by broadband stations (yellow) of the SCSN.

The project builds upon a recently completed large-scale analysis of southern California earthquake spectra (Shearer et al., 2006), to include a set of 1770 mining and other explosions between 2000 and 2005. The Shearer et al. earthquake study has already provided the largest set of earthquake spectra and stress drops computed to date, showing that individual event stress drops range between 0.2 and 20 MPa. The large number of stations and events available in southern California allows applying empirical calibration methods to remove receiver response and path propagation effects. Our efforts focus on southern California because of the unmatched size and quality of the available data, but we expect the results and insights will be applicable to other regions of more direct interest to nuclear monitoring programs. While the Shearer et al. (2006) study analyzed 1989–2001 data from short-period vertical-component stations, we examine 2000–2005 data from three-component, broadband stations. The newer data have the advantage of the horizontal components and a larger dynamic range (i.e., the older data clip on earthquakes above ~M3.5).

RESEARCH ACCOMPLISHED

The SCSN has several hundred stations and records about 12,000 to 35,000 earthquakes each year. Recently we began storing seismograms from all archived events in an online RAID system that provides rapid and random access to the data (Hauksson and Shearer, 2005). Spectra are computed as follows: For each seismogram we pick the *P* and *S* arrivals and estimate their amplitudes. This is done using the operator pick, if available, or using the output of an automatic picking algorithm for a window around the predicted arrival time (based on the catalog event location and a 1-D velocity model). Traces are resampled to a uniform 100 Hz sample rate. Spectra are computed for 1.28 s noise and signal windows, immediately before and after the pick time. We compute results for all available channels and components for both *P* and *S*, including rotation of the horizontals (if present) into transverse and radial records. Both signal and pre-event noise spectra are corrected to displacement and stored in a special binary format.

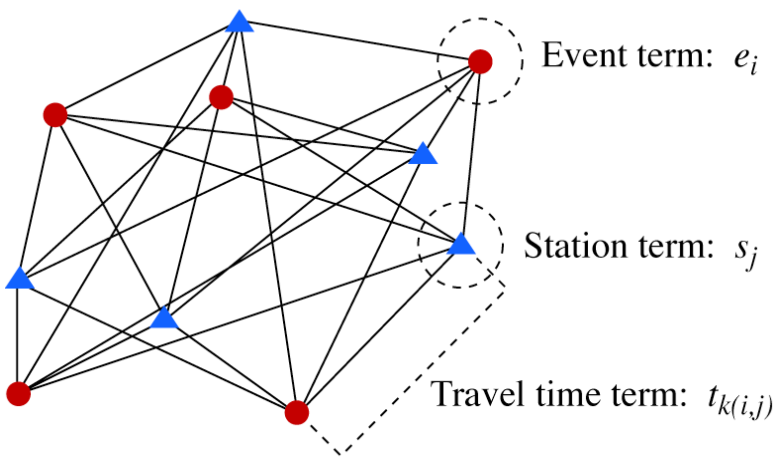

Figure 2. **A cartoon showing how measured spectra can be modeled as a product of event, station, and travel-time dependent terms.**

We apply a signal-to-noise (STN) cutoff to the spectra, requiring that the STN amplitude ratio be at least 3 for three separate bands of 5 to 10 Hz, 10 to 15 Hz and 15 to 20 Hz. Next, we process the spectra in order to isolate source, receiver and propagation path effects. This is an important step because individual spectra tend to be irregular in shape and difficult to fit robustly with theoretical models. However, by stacking and analyzing thousands of spectra it is possible to obtain more consistent results. The basic approach is illustrated in Figure 2 and is similar to that used by Warren and Shearer (2000, 2002) and Prieto et al. (2004). Each observed displacement spectrum $d_{ij}(f)$ from source i and receiver j is a product of a source term e_i (which includes the source spectrum and near-source attenuation), a near-receiver term s_j (which includes any uncorrected part of the instrument response, the site response and the near-receiver attenuation), and a travel-time dependent term $t_{k(i,j)}$ (which includes the effects of geometrical spreading and attenuation along the ray path). In the log domain, this product becomes a sum:

$$d_{ij} = e_i + s_j + t_{k(i,j)} + r_{ij} ,$$

where r_{ij} is the residual for path ij. We parameterize t in terms of the predicted P travel time between the source and receiver, using the event locations and velocity model from Lin et al. (2007). This accounts for both the event depth and the source-receiver distance. The travel-time term $t_{k(i,j)}$ is discretized by its index k at 1 s increments in travel time. Because each station records multiple events and each event is recorded by multiple stations, this is an over-determined problem. We solve this equation using a robust, iterative, least-squares method in which we sequentially solve for the terms t_k, s_j, and e_i, while keeping the other terms fixed at each stage. We suppress outliers by assigning L1-norm weights to misfit residuals greater than 0.2 s (or less than –0.2 s). This weighting scheme is necessary to ensure robustness with respect to a small number of spectra with large excursions compared to the bulk of the data. In practice we found that the method converged rapidly to a stable solution after a few iterations.

Radiation pattern differences are not included in equation (1) and would be difficult to include in our processing because they are not generally available for the smaller magnitude events. By using multiple stations for each source, however, radiation pattern effects will tend to average out. Note that this method resolves only differences in the relative shapes of the spectra. Without additional modeling assumptions, it cannot, for example, resolve how much of the spectral falloff is due to source effects and how much is due to attenuation common to all paths. The advantage of the method, however, is that it identifies and removes anomalies that are specific to certain sources or receivers. Because there may be difficulties in obtaining reliable and accurate instrument response functions for many of the stations in the archive, this is an important processing step that provides a way to correct for some of these problems.

Our focus has been on the stacked source spectra, e_i, which we ultimately use to estimate the moment and corner frequency of each event. At this stage, however, the source spectra only contain relative information among the different events. In order to estimate absolute spectra from our source stacks, we use the local magnitude M_L to obtain the scaling factor necessary to convert our relative moment estimates to absolute moment and we use an empirical Green's function approach to correct the spectral shapes for attenuation and other path effects (for details, see Shearer et al., 2006). To study the average shape of the spectra, we stack our results within equally spaced bins in the estimated seismic moment (obtained from the low-frequency part of the spectrum). Figure 3 shows these stacked spectra for both earthquakes and quarry blasts. The dashed lines show the best-fitting predictions of the ω^{-2} source model of Madariaga (1976), assuming a constant stress drop.

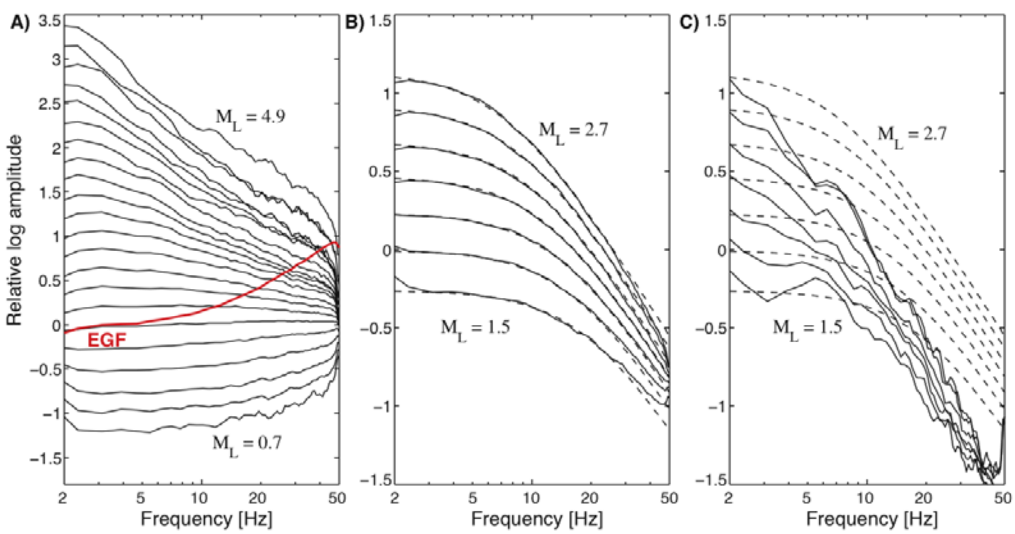

Figure 3. Stacked *P*-wave source displacement spectra from 2000 to 2005 within bins of estimated seismic moment for 17810 earthquakes and 1744 quarry blasts. (A) Stacked earthquake source terms obtained from the iterative inversion. Red line shows the empirical Green's function (EGF) used to correct these spectra for attenuation and other path effects assuming a constant stress drop model. (B) EGF corrected earthquake source terms compared to predictions of the Madariaga (1976) source model (dashed lines). (C) Stacked source terms for quarries.

Figure 3 shows that averaged earthquake spectra in southern California are well fit by a standard source model. However, the averaged quarry spectra appear anomalous in at least two respects: (1) they exhibit large misfit compared to the source model predictions, and (2) they have generally steeper falloffs at high frequencies than ω^{-2}, which will lead to lower corner frequencies and stress drop estimates. The lack of high frequency radiation from the quarries is somewhat surprising and may reflect ripple firing and/or strong near-surface attenuation. In any case, we attempt to use these two differences to discriminate between earthquakes and quarry blasts in southern California. We do this by computing the best-fitting ω^{-2} source model to the individual EGF-corrected source spectra. For each event, we obtain an estimate of the moment, the corner frequency and a measure of the root mean square (RMS) misfit to the source model. Various combinations of these parameters are plotted against each other in Figure 4. Note that the quarry blasts have generally higher misfits and smaller corner frequencies than the earthquakes. However, the two populations are not completely separated and there is some degree of overlap (see Figure 5), particularly in the corner frequency estimates.

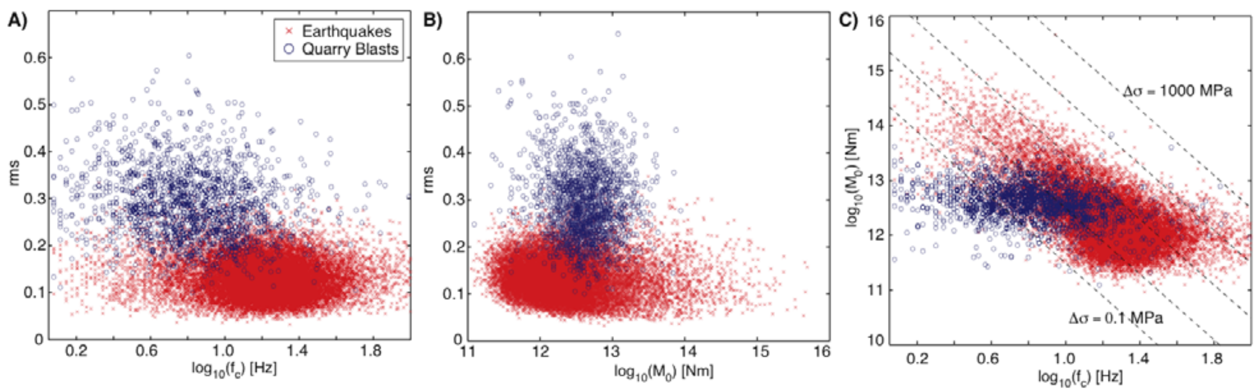

Figure 4. Earthquakes (red) and quarry blasts (blue) as a function of parameters derived from fitting their EGF-corrected spectra to an ω^{-2} source model. (A) Misfit vs. corner frequency. (B) Misfit vs. moment. (C) Moment vs. corner frequency. Stress drop estimates in (C) are from the Madariaga (1976) model.

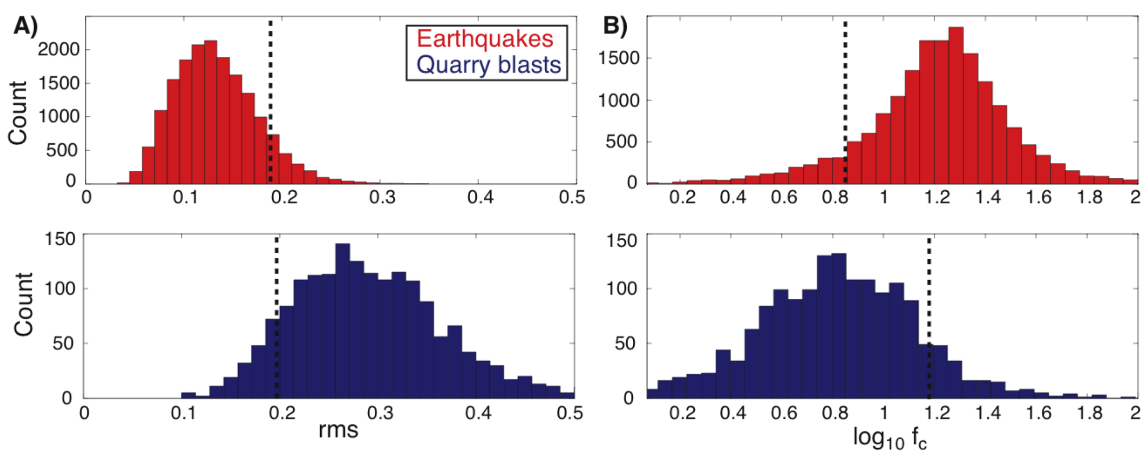

Figure 5. Histograms comparing the distribution of RMS misfit to an ω^{-2} source model (left) and corner frequency (right) for both earthquakes (red) and quarry blasts (blue). The dashed vertical lines divide the distributions into 10% and 90% parts. Note that 90% of the quarries have model misfits greater than that of 90% of the earthquakes, but that there is much more overlap in the corner frequency distributions.

In practical applications, the main interest is to discriminate between shallow earthquakes and explosions. We therefore compare the quarry blast results to earthquakes shallower than 5 km only. Although a much smaller number of events is now being used (~ 3000), the overall results of Figure 4 and 5 do not change.

Our results from analysis of *S*-wave spectra from transverse-component records have so far been inconclusive, in part because of the generally lower signal-to-noise ratios at high frequencies for the *S* waves compared to the *P* waves. However, we do observe lower average *S/P* amplitude ratios for the quarries using simple peak amplitudes in the unfiltered seismograms (Figure 6), although there is a large amount of overlap in the distributions.

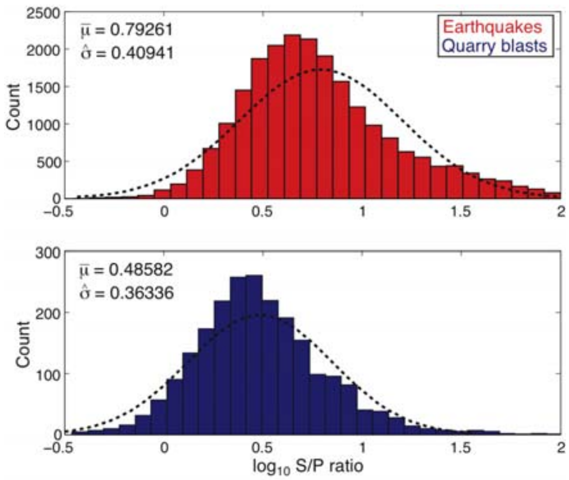

Figure 6. Histograms comparing the distributions of *S/P* amplitude ratios between earthquakes (top) and quarry blasts (bottom).

CONCLUSIONS AND RECOMMENDATIONS

Earthquakes and explosions in Southern California exhibit significant differences in their average *P*-wave spectral properties. Quarry blast spectra are not well fit by standard source models and typically have lower corner frequencies and anomalously steep falloffs at high frequencies compared to earthquakes of the same estimated moment. However, spectra from individual events have large variations and do not always permit an unambiguous identification of event type. Future results from analysis of *S*-wave spectra may provide additional discriminants.

ACKNOWLEDGEMENTS

We thank Egill Hauksson for his help in maintaining the waveform database and computing the spectra.

REFERENCES

Arrowsmith, S. J., M. D. Arrowsmith, M. A. H. Hedlin, and B. Stump (2006). Discrimination of delay-fired mine blasts in Wyoming using an automatic time-frequency discriminant, *Bull. Seismol. Soc. Am*. 96: 2368–2382, doi: 10.1785/0120060039.

Bennett, T. J. and J. R. Murphy (1986). Analysis of seismic discrimination capabilities using regional data from western United States events, *Bull. Seismol. Soc. Am*. 76: 1069–1086.

Carr, D. B. and H. D. Garbin (1998). Discriminating ripple-fired explosions with high-frequency (>16 Hz) data, *Bull. Seismol. Soc. Am*. 88: 963–972.

Gitterman, Y., V. Pinsky, and A. Shapira (1998). Spectral classification methods in monitoring small local events by the Israel seismic network, *J. Seismol*. 2: 237–256.

Gitterman, Y. and R. van Eck (1993). Spectral of quarry blasts and microearthquakes recorded at local distances in Israel, *Bull. Seismol. Soc. Am*. 83: 1799–1812.

Hartse, S. E., W. S. Phillips, M. C. Fehler, and L. S. House (1995). Single-station spectral discrimination using coda waves, *Bull. Seismol. Soc. Am*. 85: 1464–1474.

Hauksson, E. and P. Shearer (2005). Southern California hypocenter relocation with waveform cross-correlation, part 1: Results using the double-difference method, *Bull. Seismol. Soc. Am.* 95: 896–903, doi:10.1785/0120040167.

Hedlin, M. A. H. (1998). A global test of a time-frequency small-event discriminant, *Bull. Seismol. Soc. Am*. 88: 973–988.

Hedlin, M. A. H., J.-B. Minster, and J. A. O. Orcutt (1990). An automatic means to discriminate between earthquakes and quarry blasts, *Bull. Seismol. Soc. Am*. 80: 2143–2160.

Kim, W. Y., D. W. Simpson, and P. G. Richards (1994). High-frequency spectra of regional phases from earthquakes and chemical explosions, *Bull. Seismol. Soc. Am*. 84: 1365–1386.

Leidig, M.R., B.W. Stump, J.L. Bonner, C. T. Hayward, A. A. Velazco, D. F. Baker, H. Hooper, W. R. Walter, X. Yang, R. Zhou, C. L. Edwards, M. D. Renwald, and J. F. Lewkowicz (2004). Source phenomenology experiments in Arizona, in *Proceedings of the 26th Seismic Research Review: Trends in Nuclear Explosion Monitoring,* LA-UR-04-5801, Vol. 1, pp. 366–374.

Lin., G., P. M. Shearer, and E. Hauksson (2007). Applying a 3D velocity model, waveform cross-correlation, and cluster analysis to locate Southern California seismicity from 1981 to 2005, *J. Geophys. Res*. (submitted).

Madariaga, R. (1976). Dynamics of an expanding circular fault, *Bull. Seismol. Soc. Am*. 66: 639–666.

McLaughlin, K. L., J. L. Bonner, and R. Barker (2004). Seismic source mechanisms for quarry blasts: Modelling observed Rayleigh and Love wave radiation patterns from a Texas quarry, *Geophys. J. Int*. 156: 79–93.

Musil, M. and A. Plesinger (1996). Discrimination between local microearthquakes and quarry blasts by multi-layer perceptrons and Kohonen maps, *Bull. Seismol. Soc. Am*. 86: 1077–1090.

Parolai, S., L. Trojani, M. Frapiccini, and G. Monachesi (2002). Seismic source classification by means of a sonogram-correlation approach: Application to data of the RSM Seismic Network (central Italy), *Pure Appl. Geophys.* 159: 2763–2788.

Plafcan, D., E. Sandvol, D. Seber, M. Barazangi, A. Ibenbrahim, and T.-E. Cherkaoui (1997). Regional discrimination of chemical explosions and earthquakes: a case study in Morocco, *Bull. Seismol. Soc. Am*. 87: 1126–1139.

Prieto, G. A., P. M. Shearer, F. L. Vernon, and D. Kilb (2004). Earthquake source scaling and self-similarity estimation from stacking P and S spectra, *J. Geophys. Res*. 109: doi:10.1029/2004JB003084.

Shearer, P. M., G. Prieto ,and E. Hauksson (2006). Comprehensive analysis of earthquake source spectra in Southern California, *J. Geophys. Res*. 111: B06303, doi:10.1029/2005JB003979.

Smith, A. T. (1993). Discrimination of explosions from simultaneous mining blasts, *Bull. Seismol. Soc. Am*. 83: 160–179.

Stump, B., M. A. H. Hedlin, D. C. Pearson, and V. Hsu (2002). Characterization of mining explosions at regional distances, *Reviews of Geophysics* 40: 1011, doi:10.1029/1998RG000048.

Su, F., K. Aki, and N. N. Biswas (1991). Discriminating quarry blasts from earthquakes using coda waves, *Bull. Seismol. Soc. Am*. 81: 162–178.

Taylor, S. R., N. W. Sherman ,and M. D. Denny (1988). Spectral discrimination between NTS explosions and western United States earthquakes at regional distances, *Bull. Seismol. Soc. Am.* 78: 1563–1579.

Tibuleac, I. M., J. Britton, D. B. Harris, T. Hauk, H. Hooper, and J. L. Bonner (2004). Detection methods for mining explosions in southern Asia, in *Proceedings of the 26th Seismic Research Review: Trends in Nuclear Explosion Monitoring*, LA-UR-04-5801, Vol. 1, pp. 427–438.

Walter, W. R., K. M. Mayeda, and H. J. Patton (1995). Phase and spectral ratio discrimination between NTS earthquakes and explosions, part I: Empirical observations, *Bull. Seism. Soc. Am.* 85: 1050–1067.

Warren, L. M. and P. M. Shearer (2000). Investigating the frequency dependence of mantle Q by stacking P and PP spectra, *J. Geophys. Res*. 105: 25,391–25,402.

Warren, L. M. and P. M. Shearer (2002). Mapping lateral variations in upper mantle attenuation by stacking P and PP spectra, *J. Geophys. Res*. 107: B12, 2342, doi:10.1029/2001JB001195.

Wuster, J. (1993). Discrimination of chemical explosions and earthquakes in central Europe—A case study, *Bull. Seismol. Soc. Am*. 83: 1184–1212.